

In Situ Measurement of Aggregate Formation Kinetics of Nickel(II)-Pyridylazoaminophenol Complex at the Heptane-Water Interface by Centrifugal Liquid Membrane Spectrophotometry

Yoki Yulizar and Hitoshi Watarai*

Department of Chemistry, Graduate School of Science, Osaka University, Toyonaka, Osaka 560-0043

(Received December 13, 2002)

Complex formation of nickel(II) with 2-(5-bromo-2-pyridylazo)-5-diethylaminophenol (HL) and the aggregation of the monomer complex at the heptane-water interface have been kinetically studied by using centrifugal liquid membrane (CLM) spectrophotometry. The interfacial aggregation of ligand in NiL_2 complex was observed as the growth of a remarkably intense and narrow absorption band (J-band) at 588 nm, showing a bathochromic shift from the absorption maximum of the monomer complex (569 nm), accompanied by a decrease of the absorbance of the free ligand at 452 nm. The formation of aggregate was initiated when the interfacial concentration of the monomer complex attained the critical aggregation concentration (cac) of 2.4×10^{-10} mol cm^{-2}. The initial formation rate of the interfacial aggregate was proportional to concentrations of both free Ni(II) and free ligand after the attainment of cac. The observed rate constant for the aggregation, 4.1×10^{1} M^{-1} s^{-1}, was smaller than the formation rate constant of NiL_2 complex at the interface. A long period observation of the profile of absorbance change showed an oscillation of the interfacial aggregate concentration until all of the ligand was consumed, suggesting a subsequent flocculation of the aggregate in the rotating cell.

Formation and structure of molecular aggregates have become an attractive subject in various fields of chemistry.[1] H- or J-Aggregates, which refer to the molecular arrangement of face-to-face or edge-to-edge, respectively, have been reported for various organic dye systems.[2] H-Aggregates exhibit hypsochromic effect by the blue shift of H-bands, while in J-aggregates bathochromic shifts can be observed in J-bands. The red-shifted spectra of J-aggregates are caused from a strong electronic coupling of several monomers and are characterized by a narrow and intense excitonic absorption band, which is not observed in the monomer.[3] However, H-aggregates do not have such a sharp band as J-aggregates do. Complete analysis of the characteristic bands and their relation to molecular arrangement in the J-aggregate can be elucidated by a detailed investigation of their spectroscopic properties, such as absorption and emission spectra and the fluorescence life-time.[4] The structural, kinetic and spectroscopic studies on H- and J-aggregates can provide useful information for understanding molecular interactions in aggregation process.[5]

Many studies have been published on the J-aggregate formation of cyanine dyes in aqueous solution,[3,6–10] following the original studies of Scheibe[11] and Jelley.[12] Cyanine dyes adsorbed on silver halide grains[13–15] and merocyanine under UV illumination in non-polar solvent[16] showed remarkable aggregation. J-Aggregate of several porphyrins was studied in homogeneous solutions[1,17,18] or in the heterogeneous systems,[19–22] and the aggregation of xanthene dyes[23,24] was reported as well.

Aggregation and assembling of ligand molecules in metal complexes at the liquid-liquid interface is also conceivable, because at the interface of metal extraction system a two-dimensional saturation state was attained very often. However, to our knowledge, the interfacial aggregation of tetrapyridylporphine bridged by Pd(II) is the only example[25] measured at the liquid-liquid interface. There was no report in the literature on the aggregation of a Werner-type metal complex at the liquid-liquid interfaces, probably because such study of aggregate formation at interfaces requires sensitive and selective measurement techniques for the detection of the interfacial adsorption and reaction.

In this paper, we report an interfacial formation of an aggregate of bis[2-(5-bromo-2-pyridylazo)-5-diethylaminophenolato]nickel(II) complex, abbreviated as NiL_2 in the heptane-water system. A self-assembled growth of aggregate was found out by an in situ method of a centrifugal liquid membrane (CLM) spectrophotometry that has been originally developed in our laboratory.[26] By changing concentrations of the ligand and nickel ion, we could measure separately the formation rate of the metal complex and the growth rate of the aggregate at the interface with a high reproducibility. In the present study, a new extremely strong, narrow and red-shifted absorption band due to the formation of J-type aggregate at the interface was proposed.

Materials and Methods

Reagents. Heptane (Nacalai Tesque Inc., G.R.) was purified by fractional distillation after treatment with concentrated sulfuric acid for 1 day (twice), washed by water and 5% NaOH solution, and dehydrated by anhydrous $CaCl_2$ overnight. Figure 1 shows a molecular structure of pyridylazoaminophenol compound that works as a tridentate ligand. It was purchased from Dojindo and was used as received. A stock solution of Ni(II) was prepared

Published on the web July 15, 2003; DOI 10.1246/bcsj.76.1379

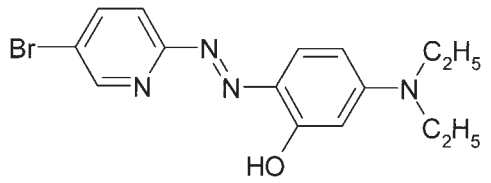

Fig. 1. Molecular structure of 2-(5-bromo-2-pyridylazo)-5-diethylaminophenol (HL).

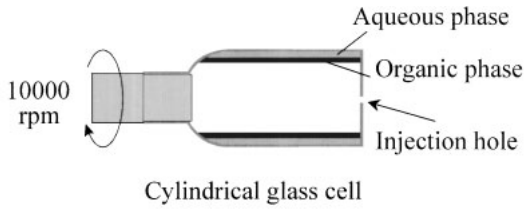

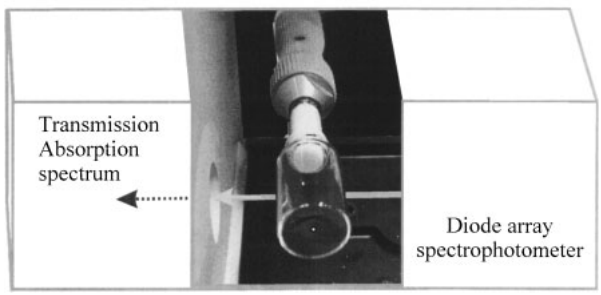

Fig. 2. Schematic drawing of the centrifugal liquid membrane (CLM) spectrophotometry. The thickness of the aqueous and organic phases were 132 μm and 80 μm, respectively, when 250 μL aqueous phase and 150 μL organic phase were used.

by dissolving pure nickel metal (>99.99%) in a small amount of perchloric acid. The pH of the aqueous phase was controlled by mixing 2-(*N*-morpholino)ethanesulfonic acid, MES (5.0×10^{-3} M) and aqueous sodium hydroxide. The ionic strength of the aqueous phase was maintained at 0.1 M by the addition of sodium perchlorate. All the reagents were of analytical reagent grade. Water was purified by using a Milli-Q system (Milli-Q Sp. TOC., Millipore) after distillation and deionization.

Observation of Microscopic Images. A heptane solution (0.150 mL) of 1.0×10^{-4} M HL and an equal volume of 5.0×10^{-3} M Ni(II) aqueous solution containing 0.1 M $(H^+, Na^+)ClO_4^-$ and MES buffer (pH 6.0) were carefully put in a cylindrical glass cell, whose inner diameter and inner height were 11 mm and 5 mm, respectively. Microscopic images of aggregates formed at the liquid-liquid interface were observed at 20, 60 and 120 minutes after the initiation of the reaction under an objective lens (45x, NA 0.55) of a microscope (Photon Design, Japan) equipped with a CCD camera and a video recording system in a thermostated room at 25 ± 1 °C.

Measurements of Interfacial Reaction. The formation reaction of nickel(II) complex at the interface was observed spectrophotometrically by CLM method shown in Fig. 2, which was analogous to the one reported previously.[27] A blank spectrum was measured at first by introducing 0.050 mL of heptane and 0.250 mL of aqueous solution containing Ni(II) ion, $(H^+, Na^+)ClO_4^-$ and MES buffer by a microsyringe into a cylindrical rotating cell. The cell was plugged by a PTFE rod, which was connected to the electronic motor (Nakanishi Inc., NK-260) and rotated at the speed of 10000 rpm. Then the complex formation was initiated by the addition of 0.100 mL of HL in heptane to the cell. The thicknesses of the aqueous phase and heptane phase under the rotation were 132 μm and 80 μm, respectively. The absorption spectra of the interface and the heptane phase were measured with a HP8452A diode array spectrophotometer or UV/VIS/NIR spectrophotometer (V-570, Jasco). The absorption spectra were recorded at the intervals of 1.0 s with the integration time of 1.0 s.

Nickel(II) concentration dependence on the observed interfacial aggregation rate was studied by varying the concentrations of Ni(II) in the range from 1.0×10^{-5} to 1.0×10^{-3} M at the constant HL concentration of 6.7×10^{-5} M. HL concentration dependence on the rate was measured at the constant Ni(II) concentration of 1.0×10^{-3} M, while the concentration of HL was changed in the range of 2.5×10^{-5} to 1.0×10^{-4} M. The pH value of aqueous phase was fixed at 6.00 ± 0.04.

Results and Discussion

Microscopic Images. When the organic phase was placed on the aqueous phase in a cylindrical glass, the aggregate of nickel(II) complex was formed at the heptane-water interface. This was directly observed by a microscope objective located just above the liquid-liquid interface. The aggregate growth observed at the interface is shown in Fig. 3. According to the time course, Fig. 3a (observed at 20 minutes) showed the formation of a thin layer of aggregate. At 60 min (Fig. 3b), a large segment started to appear that indicated an interaction among the aggregates. The image (Fig. 3c) at 120 min depicted the network-like accumulate of the aggregate. The average population and the growth rate of the accumulate decreased with decreases in both Ni(II) ion and HL concentrations.

Interfacial Formation of J-aggregate of Nickel(II) Complex. In the previous paper, we have reported that some Ni(II) complex was extracted in heptane in a batch system showing an absorption maximum at 511 nm.[28] In the present study, the spectrum observed by CLM method showed two absorption maxima at 530 nm and 569 nm during 10–200 s after the initiation of the reaction. These maxima were assigned to the NiL_2 monomer adsorbed at the heptane-water interface.[28] After 200 s, the maxima at 530 nm and 569 nm shifted gradually to 549 nm and 588 nm (Fig. 4). This bathochromic shift was assigned to the interfacial formation of the aggregate of monomer complexes $(NiL_2)_n$. We took into account the result that an aggregation of ligands in the complexes could show an exciton splitting in excited states in the aggregate, if it has sufficiently strong electronic transition in the ligand molecules.[29] The peak at 588 nm is an intense and narrow absorption band, which has larger molar absorptivity, $\varepsilon = 4.66 \times 10^5\ M^{-1}\,cm^{-1}$, with respect to the monomer complex, $\varepsilon = 1.46 \times 10^5\ M^{-1}\,cm^{-1}$ at 569 nm. This is a characteristic feature for J-aggregate. The narrow band could be due to the delocalized excitonic states of ligands in the aggregates generated by the stacking between the ligands.

Process of J-aggregate Growth. The spectral change caused by the interfacial aggregation of nickel(II) complex is shown in Fig. 4 under the conditions of 4.9×10^{-5} M HL, 1.0×10^{-3} M Ni(II) and pH 6.0. Immediately after the initiation of the reaction, the formation of NiL_2 monomer (569 nm) was observed. When the interfacial concentration of the

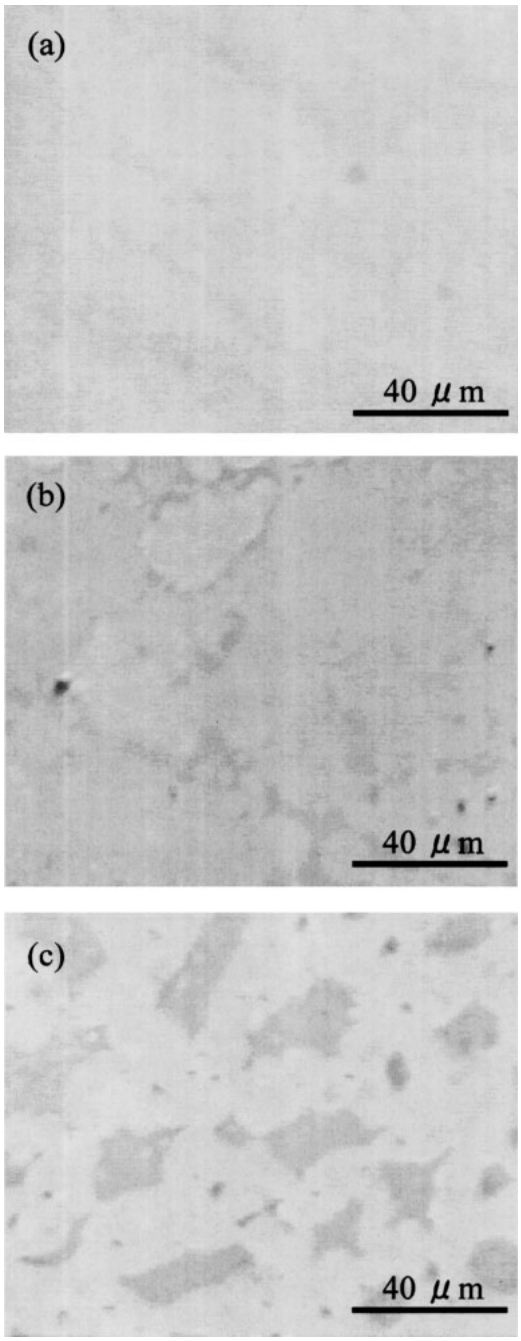

Fig. 3. Microscopic image of aggregate growth of nickel(II) complex at the heptane-water interface (a) 20 min, (b) 60 min, and (c) 120 min after the contact of two phases; [HL] $= 1.0 \times 10^{-4}$ M, [Ni(II)] $= 5.0 \times 10^{-3}$ M, pH 6.0.

monomer complex reached a critical concentration, the maximum at 569 nm shifted to a new excitonic narrow band (J-band) at 588 nm, which was attributable to the aggregate formation overlapped with the ligands. The critical concentration was defined as a critical aggregation concentration (cac) $[NiL_2]_i^c$.

Figure 5 shows the kinetic profile of the interfacial complexation and aggregation of NiL_2 complex measured at fixed wavelengths. The absorbance of HL at 452 nm gradually decreased, while the absorbance of NiL_2 monomer observed

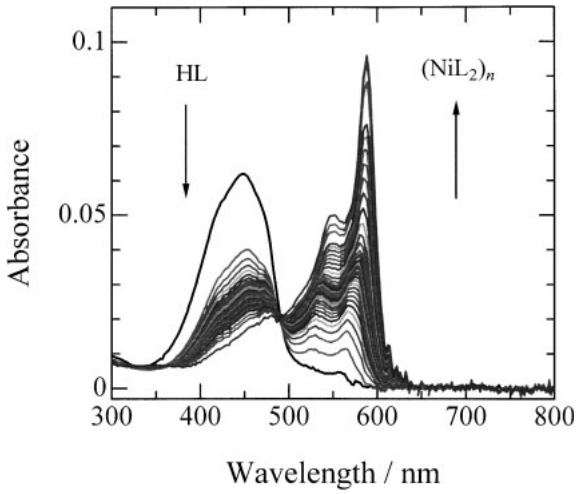

Fig. 4. The spectral change of the interfacial complex of NiL_2 at heptane-water interface observed by CLM method. The absorption spectra were recorded at 10 s intervals until the equilibrium was attained (500 s); $[HL]_T = 4.9 \times 10^{-5}$ M, $[Ni(II)]_T = 1.0 \times 10^{-3}$ M, pH 6.0.

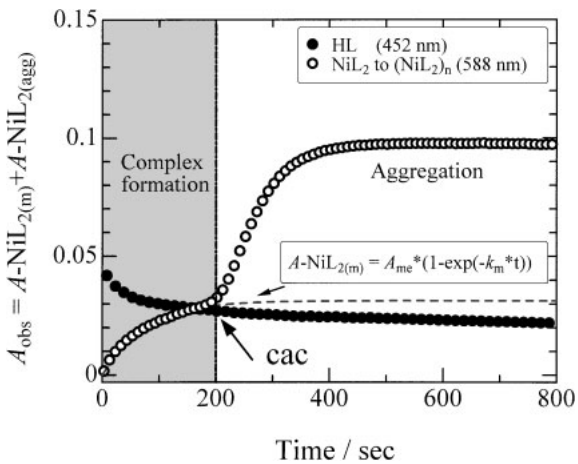

Fig. 5. Absorbance decrease of the ligand at 452 nm and absorbance increase of the interfacial aggregate of NiL_2 complex at 588 nm. The dashed line is the fitted one for the NiL_2 monomer complex formation until the critical aggregation concentration (cac) using a pseudo first-order kinetic equation. Experimental conditions are the same with those of Fig. 4.

at 588 nm increased simultaneously. Immediately after the critical aggregation concentration was attained at 200 s, a rapid increase in the absorbance due to the interfacial aggregation was observed at 588 nm.

The Y-axis, A_{obs}, in Fig. 5 includes both absorbances of NiL_2 monomer, $A\text{-}NiL_{2(m)}$, and its aggregate, $A\text{-}NiL_{2(agg)}$, at 588 nm:

$$A_{obs} = A\text{-}NiL_{2(m)} + A\text{-}NiL_{2(agg)} \quad (1)$$

where subscripts m and agg indicate the monomer and the aggregate, respectively.

The formation rate of NiL_2 monomer was analyzed using a pseudo first-order kinetic equation:

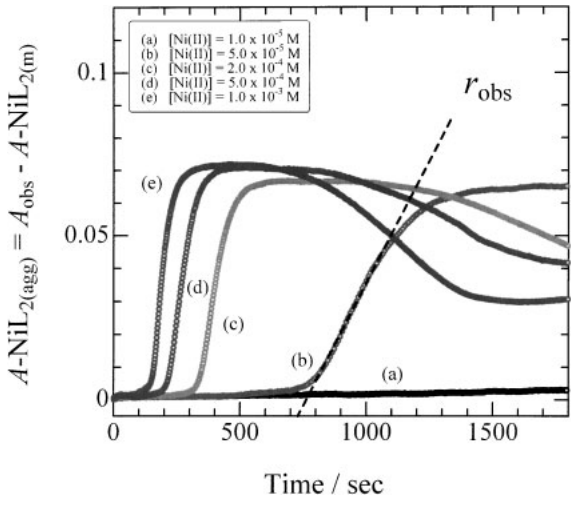

Fig. 6. Kinetic profiles of the interfacial aggregation after the correction for the monomer complex formation; $[HL]_T = 6.7 \times 10^{-5}$ M, $[Ni(II)]_T = 1.0 \times 10^{-5}$–$1.0 \times 10^{-3}$ M, pH 6.0.

$$A\text{-NiL}_{2(m)} = A_{me}(1 - \exp(-k_m t)) \quad (2)$$

where A_{me} referred to the absorbance of the monomer complex at the critical aggregation concentration and k_m is the observed interfacial formation rate constant of NiL_2. These values were calculated as $A_{me} = 3.14 \times 10^{-2}$ at 588 nm and $k_m = 1.39 \times 10^{-2}$ s^{-1}, respectively. The value of A_{me} was used for the calculation of cac by this equation:[26]

$$[NiL_2]_i^c = \frac{A_{me}}{2}\frac{1}{10^3\varepsilon} \quad (3)$$

Here, ε was the molar absorptivity for NiL_2 complex at the interface at 588 nm measured by CLM method. The value of $\varepsilon = 6.5 \times 10^4$ M^{-1} cm^{-1} was obtained from the slope of the plot of the absorbance of NiL_2 complex at 588 nm against the ligand concentration; it was performed at the concentration of Ni(II) 1.0×10^{-3} M and pH 6.0 (figure is not shown). Using this value, we obtained the value of critical aggregation concentration $[NiL_2]_i^c = 2.4 \times 10^{-10}$ mol cm^{-2}.

The profile of net growth of the aggregate was obtained by subtracting from A_{obs} with the absorbance of the monomer complex as shown in Figs. 6 and 7. They show clearly a specific retardation time for the aggregation that depends on both concentrations of Ni(II) and HL.

Figure 6 shows the kinetic profiles of the interfacial aggregation of NiL_2 complex at various concentrations of Ni(II) ion. Figure 6a did not show any aggregation at all at the low concentration of Ni(II) ion ($<5.0 \times 10^{-5}$ M) under the fixed concentration of HL 6.7×10^{-5} M and pH 6.0. At the higher concentration of Ni(II) ion ($\geq 5.0 \times 10^{-5}$ M), however, the aggregation was observed (Fig. 6b). The increase of Ni(II) concentration made the retardation time for the aggregation shorter, as shown in Figs. 6c, d and e.

Figure 7 shows the kinetic profiles of the interfacial aggregation at various concentrations of the ligand. At low concentration of HL ($<2.9 \times 10^{-5}$ M) under the fixed concentration of $[Ni(II)] = 1.0 \times 10^{-3}$ M and pH 6.0, only monomer NiL_2 complex was formed at the interface (Fig. 7a). At the relatively high concentration of HL ($\geq 2.9 \times 10^{-5}$ M), in contrast, the formation of aggregate (at 588 nm) was observed from 700 s after the beginning of the measurements, as shown in Fig. 7b. Further increase of HL concentration shortened the retardation time and increased the rate of aggregation, as shown in Figs. 7c, d, e and f.

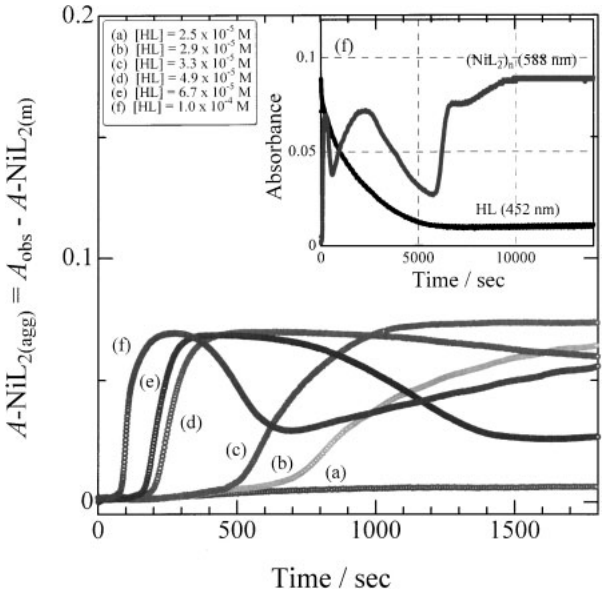

Fig. 7. Kinetic profiles of the aggregate growth at the interface. The inset figure shows the interfacial reaction until all of the ligand was consumed to form aggregate until 14000 s; $[HL]_T = 2.5 \times 10^{-5}$–$1.0 \times 10^{-4}$ M, $[Ni(II)]_T = 1.0 \times 10^{-3}$ M, pH 6.0.

The maximum absorbance of the aggregate at the condition of 3.3×10^{-5} M HL did not change until 1800 s after attaining the equilibrium state (see Fig. 7c). In the formation of pseudoisocyanine (PIC) J-aggregates in aqueous solution, it has been assumed that the number of PIC molecules in the J-aggregate has to increase in the process of growth and has to be greater in solutions of higher concentration.[6,7] However, in this study, the maximum absorbance was not changed at the HL concentration higher than 4.9×10^{-5} M (Fig. 7). Such a result suggested the saturation of the interfacial aggregate. After the attainment of the saturated value, a decrease of absorbance was observed at the higher HL concentrations (Figs. 7d, e and f). A similar decrease was observed in the higher Ni(II) concentration, as shown in Figs. 6c, d and e. In all the interfacial aggregation measurements, the absorbance maximum of the aggregate at 588 nm was the same for any concentrations of the reactants. A decrease of the absorbance after the saturation suggested that the aggregate made a flocculation that proceeded to crystal formation. As shown in Fig. 7 (inset), the absorbance oscillated versus time for the prolonged measurement until 14000 s. Probably, the aggregation and flocculation processes occurred alternatively until all of the ligand was consumed. The mechanism of the self-assembling of NiL_2 monomer complex into large supramolecular aggregates at heptane-water interface was postulated, as shown in Fig. 8.

Interfacial Aggregation Kinetics. From the corrected

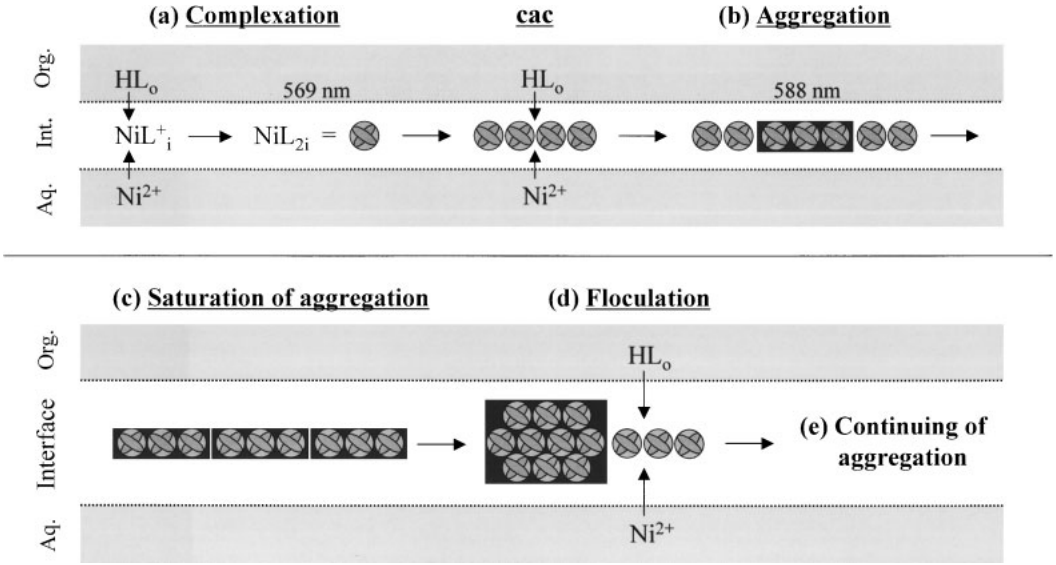

Fig. 8. Schematic representation of the interfacial aggregation mechanisms of the monomer complex into supramolecular aggregate of NiL_2 complex at heptane-water interface. (a) Formation of monomer NiL_{2i} complex at the interface, represented by a gray circle including crossed ovals. (b) Interfacial aggregate growth after the attainment of cac. (c) The interfacial concentration of the aggregate reaches the saturated aggregation condition in a cell interface. (d) The aggregate makes a flocculation, which may proceed to a crystal formation. (e) And the aggregation growth still took place at the interface until all of the ligand is consumed.

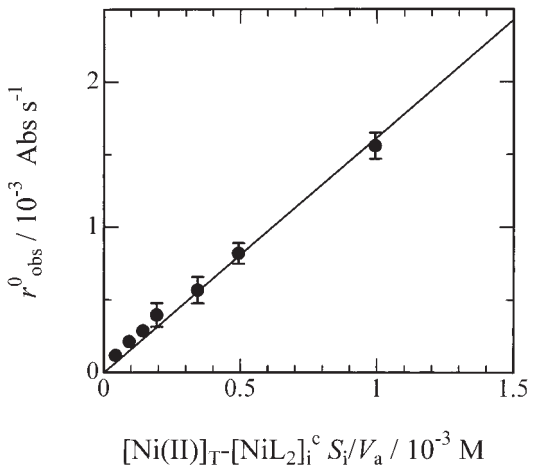

Fig. 9. Dependence of the observed initial rate for the interfacial aggregation, r^0_{obs} on the free Ni(II) concentration; $[HL]_T = 6.7 \times 10^{-5}$ M, $[Ni(II)]_T = 5.0 \times 10^{-5}$–$1.0 \times 10^{-3}$ M, pH 6.0.

absorbance change at 588 nm for the interfacial aggregation (Figs. 6 and 7), the observed initial formation rate of the aggregate (r^0_{obs}) was obtained by a least squares regression, as shown in Fig. 6b.

Figure 9 shows the Ni(II) concentration dependence on the observed initial rate of the interfacial aggregation. Considering that the aggregation started at the time of cac, we calculated the concentration of Ni(II) ion at the cac, $[Ni(II)]_0$, by,

$$[Ni(II)]_0 = [Ni(II)]_T - [NiL_2]_i^c S_i/V_a \quad (4)$$

where subscripts T and V_a refer to the total concentration and the volume of aqueous phase, respectively. The observed initial formation rate of the interfacial aggregate increased with the increase in the nickel(II) concentration with a linear correlation.

Figure 10 shows the dependence of r^0_{obs} on the HL concentration in the organic phase at cac. We calculated the concentration of HL at cac, $[HL]_0$, by the equation:

$$[HL]_0 = [HL]_T - 2[NiL_2]_i^c S_i/V_o \quad (5)$$

Figure 10 showed a saturation curve just like an adsorption isotherm. Therefore, we calculated the interfacial HL concentration, $[HL]_i$, by a Langmuir isotherm, assuming that the interfacial adsorption of HL was not interfered with by the presence of the interfacial complex,

$$[HL]_i = \frac{aK'[HL]_o}{a + K'[HL]_o} \quad (6)$$

where a and K' are the saturated interfacial concentration of HL and the interfacial adsorption constant for HL, respectively. The plot of r_{obs} against $[HL]_i S_i/V_o$ gave a linear correlation, as shown in Fig. 10 (inset).

We thought that the first step of the reaction in the heptane–water system was the complexation reaction at the interface, which produced NiL_2 complex. The next step was assumed to be the interfacial formation of the aggregate $(NiL_2)_{ni}$ from the monomer complex:

$$HL_o \overset{K'}{\rightleftharpoons} HL_i \quad (7)$$

$$Ni^{2+} + 2HL_i \rightarrow NiL_{2i} + 2H^+ \quad (8)$$

$$nNiL_{2i} \overset{K_{agg}}{\rightleftharpoons} (NiL_2)_{ni} \quad (9)$$

From the experimental results, the rate law for the formation of the aggregate was determined as

$$r^0_{obs} = \frac{nd[(NiL_2)_n]_i}{dt}\frac{S_i}{V_o} = k_{agg}[Ni(II)][HL]_i\frac{S_i}{V_o} \quad (10)$$

This means that the rate-determining step is the formation of

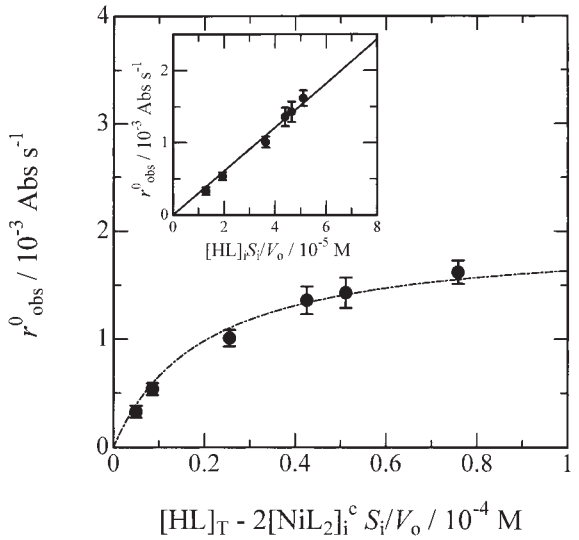

Fig. 10. Correlation of the observed initial rate for the interfacial aggregation, r^0_{obs} to the free HL concentration. The inset figure shows the r^0_{obs} against the interfacial HL concentration calculated by the Langmuir isotherm; $[HL]_T = 2.9 \times 10^{-5}$–$1.0 \times 10^{-4}$ M, $[Ni(II)]_T = 1.0 \times 10^{-3}$ M, pH 6.0.

1:1 complex, as was the case in the formation of monomer complex, NiL_2. Taking into account that the aggregation occurred after the cac, we could represent the initial rate for the aggregation by

$$r^0_{obs} = k_{agg}([Ni(II)]_T - [NiL_2]_i^c S_i/V_a)\left(\frac{aK'[HL]_o}{a + K'[HL]_o} S_i/V_o\right)2\varepsilon l \quad (11)$$

where $[HL]_0$ was defined by Eq. 5. From the slope of Fig. 9, we could obtain the interfacial aggregation rate constant, $k_{agg} = 4.45 \times 10^1$ $M^{-1}\,s^{-1}$, by using the values of $\log(a/\text{mol cm}^{-2}) = -10.29$,[30] $K' = 2.59 \times 10^{-3}$ cm for HL at heptane-water interface and $2\varepsilon l = 8.29 \times 10^3$ M^{-1} (at 588 nm) for NiL_2 aggregate at the interface. In the same way, from the slope of Fig. 10 (inset) and the above values, we obtained $k_{agg} = 3.70 \times 10^1$ $M^{-1}\,s^{-1}$. Therefore, the averaged value of the aggregation rate constant at the heptane-water interface was $k_{agg} = 4.1 \times 10^1$ $M^{-1}\,s^{-1}$. This value is significantly smaller than that of the interfacial formation rate constant of the monomer complex, $k_i = 1.1 \times 10^2$ $M^{-1}\,s^{-1}$.[28] This means that the reaction probability of 1:1 complex formation in the aggregation is reduced by the factor of 2.7 from the monomer complexation. This might be attributable to the occupation of the interface by the monomer complex at the critical aggregation concentration.

Aggregation Number and Probable Models. To determine the average aggregation number, n, the reaction of Eq. 9 was used for the interfacial aggregate formation from monomer complex. K_{agg} is the equilibrium aggregation constant, defined by

$$K_{agg} = \frac{[(NiL_2)_n]_i}{[NiL_2]_i^n} \quad (12)$$

where $[(NiL_2)_n]$ refers to the concentration of NiL_2 forming the aggregate.

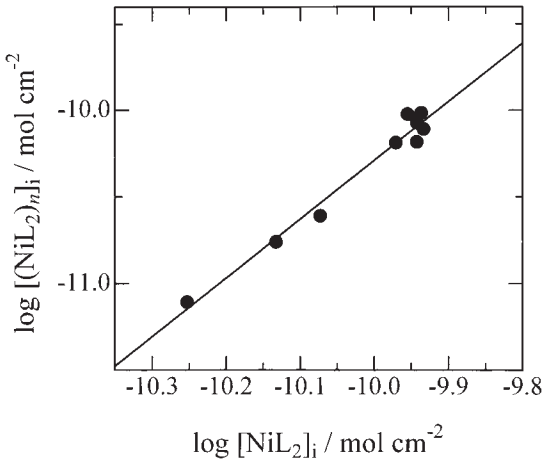

Fig. 11. Logarithmic plot of the interfacial NiL_2 concentration in the aggregate, $[(NiL_2)_n]_i$ against that of the free interfacial monomer complex, $[NiL_2]_i$ at the equilibrium state. The slope of the straight line was 3.0.

Equation 12 can be changed to the following equation:

$$\log[(NiL_2)_n]_i = \log K_{agg} + n \log[NiL_2]_i \quad (13)$$

The interfacial concentrations of monomer complex, $[NiL_2]_i$ and the aggregate, $[(NiL_2)_n]_i$ were calculated from the absorbance at the saturated state of the aggregate using Eq. 3, where $\varepsilon = 1.46 \times 10^5$ $M^{-1}\,cm^{-1}$ at 569 nm and $\varepsilon = 4.66 \times 10^5$ $M^{-1}\,cm^{-1}$ at 588 nm were used for NiL_2 complex and its aggregate, respectively. Figure 11 shows the linear relationship between the interfacial concentrations of aggregate and monomer complex. From this figure was obtained the value of the aggregation number, $n = 3$, and the stability constant of aggregation, $\log K_{agg} = 23.7$ $mol^{-2}\,cm^4$. The large value of K_{agg} indicated that the aggregate formation from the monomer complex proceeded spontaneously at the interface after the attainment of the cac.

Figure 12 shows probable models for the aggregation of monomer complex NiL_2 at the interface, where one Ni(II) ion binds 2 ligands with (N, N, O) coordination. At the cac, 3 complex molecules occupy 3 unit-areas, as denoted by 3/3 in Fig. 12a. The monomer complex will be arranged in a way that produces stacking through interaction between pyridylazoaminophenol ligands to form aggregates. We proposed two kinds of model for interfacial aggregate of NiL_2 complex, as shown in Figs. 12b and 12c, these had probable saturation aggregation states of 2/3 and 1.5/3 (3 complex molecules occupied 2 and 1.5 unit-areas, respectively). From the experimental results (see Figs. 6 and 7), we calculated the value of the absorbance maximum for the aggregate at the interface, $A\text{-}NiL_{2i(agg)}{}^{max}$, to be $(7.09 \pm 0.14) \times 10^{-2}$. This value was used to calculate the concentration of NiL_2 in the interfacial aggregate at the saturated situation using Eq. 3, and it was obtained as $[(NiL_2)_n]_i{}^{sat} = (7.61 \pm 0.15) \times 10^{-11}$ mol cm^{-2}. This value was 0.32 times that of cac, supporting the probable saturation state of 1.5/3. Therefore, in the present study we proposed that the aggregate of NiL_2 complex had a structure shown in Fig. 12c. This figure shows the molecular arrangement schematically, in which the ligand plane has a relatively small orienta-

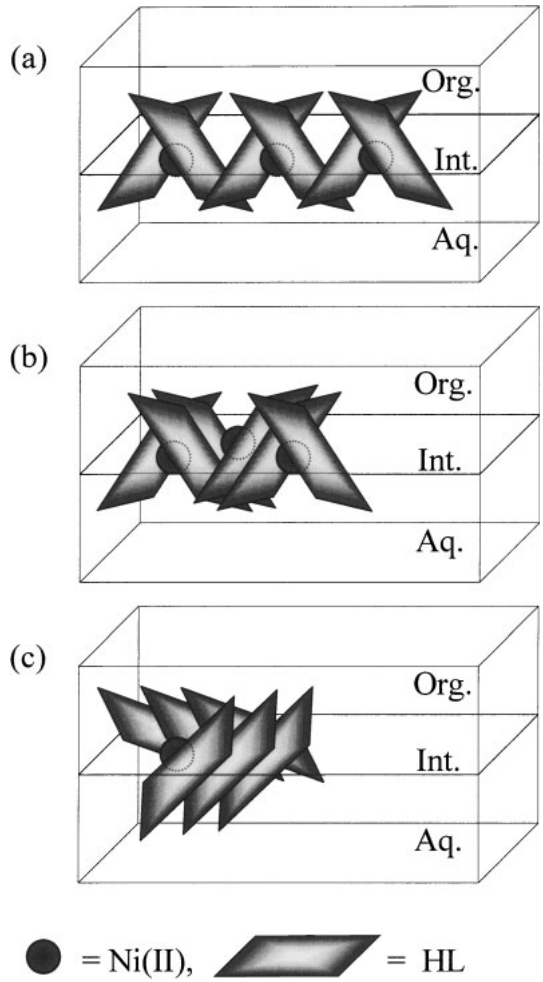

Fig. 12. Probable models for the interfacial aggregation of NiL_2 monomer complexes. (a) No stacking, (b) One ligand in a complex is stacking with the ligand of the different complex, (c) Two ligands of a complex are stacking with the two ligands of the neighbored complex.

tion angle to the interface and the ligand is stacking with the ligand of the adjacent complex.

The molecular configuration in H- and J-type aggregate could be predicted by the extended dipole model, which was proposed by Kuhn and co-workers for the first time.[31] According to their treatment, the ligand molecules are replaced by extended dipoles of length l and charges $+q$ and $-q$. The extended dipole length and the charge are assumed to be related to the transition dipole moment of the ligand μ as $\mu = ql$. The energy shift ($\Delta E'$) between two extended dipoles is obtained as[32]

$$\Delta E' = \frac{2q^2}{D}\left(\frac{1}{r_1} + \frac{1}{r_2} - \frac{1}{r_3} - \frac{1}{r_4}\right) \tag{14}$$

where D is the dielectric constant of medium ($D = 1.92$ for heptane) and r_i is the distance between two charges. Thus for n-mer aggregate, the $\Delta E'$ value between ith and jth ligand molecules is given as[32]

$$\Delta E' = \frac{2q^2}{D}\sum_{i\neq j}^{n}\left(\frac{1}{|r_i^+ - r_j^+|} + \frac{1}{|r_i^- - r_j^-|} - \frac{1}{|r_i^+ - r_j^-|} - \frac{1}{|r_i^- - r_j^+|}\right) \tag{15}$$

where $|r_i^+ - r_j^+|$, $|r_i^- - r_j^-|$, $|r_i^+ - r_j^-|$ and $|r_i^- - r_j^+|$ are the distances between two positive charges, two negative charges and between opposite charges of ith and jth molecules, respectively. The excitation energy of the absorption maximum for an aggregate ΔE_{agg} is approximated from the excitation energy of monomer peak ΔE_m and the interaction integral $\Delta E'$ as

$$\Delta E_{agg} = \Delta E_m \pm \Delta E' \tag{16}$$

The charge of the nitrogen atom that binds the diethyl group is assumed as $+q$ and the charge of $-q$ lies at the nitrogen atom in pyridyl ring. The values of $\Delta E'$ are calculated by using the dipole length of pyridylazoaminophenol ligand $l = 8.4$ Å and by estimating the distance between adjacent molecular dipoles at 6.5 Å; these values assume similarity to pseudoisocyanine molecules in J-aggregate.[33] Varying the slip angle α from the transition dipole moments of ligand to their center-to-center lines of the aggregate gave the values of energy shift $\Delta E'$. The observed energy shift of the aggregate from nickel(II) monomer complex was $\Delta E' = -0.07$ eV. The value of $\Delta E'$ with molecules number $n = 3$ suggested a slip angle α of 35°; this value supported the edge-to-edge arrangement between ligand molecules in complex aggregate.

Conclusion

In the present study, the distinguished potential of centrifugal liquid membrane (CLM) spectrophotometry was successfully applied for the elucidation of interfacial aggregation kinetics in the reaction of nickel(II) with pyridylazoaminophenol compound at the liquid-liquid interface. The absorption spectrum of the aggregate showed a sharp and narrow band with a red shift from 569 nm (monomer complex) to 588 nm. We proposed that the aggregate was formed from three NiL_2 monomer complexes (trimer) in a close packed layer that oriented at the interface with a slip angle $\alpha = 35°$ between the transition dipole moments of ligand to their center-to-center lines. The critical aggregation concentration (cac) was defined for the first time and the value was determined to be $[NiL_2]_i^c = 2.4 \times 10^{-10}$ mol cm^{-2} in the aggregation of nickel(II) complex at the interface. The rate of aggregate formation was linearly dependent on concentrations of both free nickel(II) ion and free ligand. In this study, we have further observed an interesting oscillation phenomenon in the aggregate growth after the whole interface was covered by the aggregate, suggesting an alternative process of flocculation of aggregate and aggregate formation again until all of the ligands were consumed at the interface.

This work was financially supported by a Grant-in-Aid for Scientific Research (A) (No. 12304045) and a Scientific Research of Priority Area (No. 13129204) from the Ministry of Education, Culture, Sports, Science and Technology.

References

1 D. L. Akins, H.-R. Zhu, and C. Guo, *J. Phys. Chem.*, **100**, 5420 (1996).

2 N. Micali, F. Mallamace, A. Romeo, R. Purrello, and L. M. Scolaro, *J. Phys. Chem. B*, **104**, 5897 (2000).

3 W. J. Harrison, D. L. Mateer, and G. J. T. Tiddy, *J. Phys. Chem.*, **100**, 2310 (1996).

4 L. K. Gallos, A. V. Pimenov, I. G. Scheblykin, M. Van der Auweraer, G. Hungerford, O. P. Varnavsky, A. G. Vitukhnovsky, and P. Argyrakis, *J. Phys. Chem. B*, **104**, 3918 (2000).

5 N. C. Maiti, S. Mazumdar, and N. Periasamy, *J. Phys. Chem. B*, **102**, 1528 (1998).

6 I. Struganova, *J. Phys. Chem. A*, **104**, 9670 (2000).

7 H. von Berlepsch, C. Bottcher, and L. Dahne, *J. Phys. Chem. B*, **104**, 8792 (2000).

8 F. Rotermund, R. Weigand, and A. Penzkofer, *Chem. Phys.*, **220**, 385 (1997).

9 M. Mauerer, A. Penzkofer, and J. Zweck, *J. Photochem. Photobiol., B*, **47**, 68 (1998).

10 H. von Berlepsch, C. Bottcher, A. Ouart, C. Burger, S. Dahne, and S. Kirstein, *J. Phys. Chem. B*, **104**, 5255 (2000).

11 G. Scheibe, *Angew. Chem.*, **49**, 563 (1936).

12 E. E. Jelley, *Nature*, **138**, 1009 (1936).

13 H. Asanuma and T. Tani, *J. Phys. Chem. B*, **101**, 2149 (1997).

14 J. E. Maskasky, *Langmuir*, **7**, 407 (1991).

15 J. E. Maskasky, *J. Imaging Sci.*, **35**, 29 (1991).

16 P. Uznanski, *Synth. Met.*, **109**, 281 (2000).

17 N. Micali, L. M. Scolaro, A. Romeo, and F. Mallamace, *Phys. Rev. E: Stat. Phys., Plasmas, Fluids, Relat. Interdiscip. Top.*, **57**, 5766 (1998).

18 F. Mallamace, L. M. Scolaro, A. Romeo, and N. Micali, *Phys. Rev. Lett.*, **82**, 3480 (1999).

19 D. C. Barber, R. A. Freitag, and D. G. Whitten, *J. Phys. Chem.*, **95**, 4074 (1991).

20 O. Ohno, Y. Kaizu, and H. Kobayashi, *J. Chem. Phys.*, **99**, 4128 (1993).

21 R.-H. Jin, S. Aoki, and K. Shima, *J. Chem. Soc., Faraday Trans.*, **93**, 3945 (1997).

22 R. F. Pasternack, E. J. Gibbs, P. J. Collings, J. C. dePaula, L. C. Turzo, and A. Terracina, *J. Am. Chem. Soc.*, **120**, 5873 (1998).

23 J. E. Selwyn and J. I. Steinfeld, *J. Phys. Chem.*, **76**, 762 (1972).

24 P. R. Ojeda, I. A. K. Amashta, J. R. Ochoa, and I. L. Arbeloa, *J. Chem. Soc., Faraday Trans. 2*, **84**, 1 (1988).

25 N. Fujiwara, S. Tsukahara, and H. Watarai, *Langmuir*, **17**, 5337 (2001).

26 H. Nagatani and H. Watarai, *Anal. Chem.*, **70**, 2860 (1998).

27 Y. Yulizar, A. Ohashi, H. Nagatani, and H. Watarai, *Anal. Chim. Acta*, **419**, 107 (2000).

28 Y. Yulizar, A. Ohashi, and H. Watarai, *Anal. Chim. Acta*, **447**, 247 (2001).

29 M. Kasha, H. R. Rawls, and M. Ashraf El-Bayoumi, *Pure Appl. Chem.*, **11**, 371 (1965).

30 H. Watarai and F. Funaki, *Langmuir*, **12**, 6717 (1996).

31 V. Czikkely, H. D. Foresterling, and H. Kuhn, *Chem. Phys., Lett.*, **6**, 207 (1970).

32 A. Miyata, Y. Unuma, and Y. Higashigaki, *Bull. Chem. Soc. Jpn.*, **64**, 2786 (1991).

33 H. Yao, R. Kawabata, H. Ikeda, and N. Kitamura, *Phys. Chem. Chem. Phys.*, **1**, 4629 (1999).